Mapping of the thermodynamic performance of the supercritical CO2 cycle and optimisation for a small modular reactor and a sodium-cooled fast reactor

Hong-Son Pham, Nicolas Alpy, Jean-Henry Ferrasse, Olivier Boutin, J. Quenaut, Mark Tothill, David Haubensack, M. Saez

▶ **To cite this version:**

Hong-Son Pham, Nicolas Alpy, Jean-Henry Ferrasse, Olivier Boutin, J. Quenaut, et al.. Mapping of the thermodynamic performance of the supercritical CO2 cycle and optimisation for a small modular reactor and a sodium-cooled fast reactor. Energy, 2015, 87, pp.412-424. 10.1016/j.energy.2015.05.022 . hal-01297663

HAL Id: hal-01297663
https://hal.science/hal-01297663

Submitted on 23 Apr 2024

HAL is a multi-disciplinary open access archive for the deposit and dissemination of scientific research documents, whether they are published or not. The documents may come from teaching and research institutions in France or abroad, or from public or private research centers.

L'archive ouverte pluridisciplinaire **HAL**, est destinée au dépôt et à la diffusion de documents scientifiques de niveau recherche, publiés ou non, émanant des établissements d'enseignement et de recherche français ou étrangers, des laboratoires publics ou privés.

Mapping of the thermodynamic performance of the supercritical CO_2 cycle and optimisation for a small modular reactor and a sodium-cooled fast reactor

H.S. Pham[a,*], N. Alpy[a], J.H. Ferrasse[b], O. Boutin[b], J. Quenaut[c], M. Tothill[c], D. Haubensack[a], M. Saez[a]

a CEA Cadarache, DEN/DER/SESI/LE2S, FR-13108 Saint-Paul-lez-Durance, France
b Aix-Marseille Universite, CNRS, ECM, M2P2 UMR 7340, FR-13451 Marseille, Frane
c ALSTOM, Brown Boveri Strasse 7, CH-5401 Baden, Switzerland

The supercritical CO_2 (sc-CO_2) cycle is being promoted worldwide by many R&D energy organisations and companies as an alternative to the Rankine steam cycle for its capacity to deliver high performance, simple and compact power conversion systems. The past decade has seen an extensive number of published studies carried out in view of analysing the advantages of this cycle for various applications, from nuclear to solar energies. In that context, this work first reports a mapping of the thermodynamic performance of different sc-CO_2 cycle configurations that encompass a 250–850 °C TIT (turbine inlet temperature) range. The main compressor inlet temperature was chosen to be 35 °C to accommodate various heat-sink temperatures while the maximum pressure was parameterised at 20 MPa and at 25 MPa. These charts are seen to provide a preliminary engineering guideline to the maximum performance that one can expect from a sc-CO_2 cycle coupled to a specific application. Additionally, they illustrate the effect of the interlinked constraints in terms of optimal recuperation power and IHX (Intermediate Heat eXchanger) inlet temperature.

Following this generic study, two typical nuclear applications have been investigated with the support of an exergy analysis. A SMR (small modular reactor) featuring a current generation Pressurized Water Reactor has been chosen as an example of a low temperature range case. Parametric studies of a recompression cycle featuring a TIT of 275 °C have guided investigations regarding optimal operating conditions depending on a balance between cycle efficiency, recuperation power, and main compressor operation margin with respect to the critical point. Options for performance improvement such as reheat and condensing mode operation have been investigated for a maximum cycle pressure of 20 MPa. Thermal efficiencies of 29.3% and 28.6% respectively are reported for these two cases. This is in contrast to 27.1% for the initial recompression cycle design. Even though the penalty when compared to a Rankine steam cycle is significant, the sc-CO_2 cycle in condensing mode is viewed as an interesting option thanks to its system simplicity and footprint saving.

Moving to a higher temperature range, the sc-CO_2 cycle has been studied at a TIT of 515 °C for a test case application to a SFR (sodium-cooled fast reactor). The recompression cycle operating at a compressor inlet temperature of 35 °C provides a maximum efficiency of 43.9% and features an optimal IHX inlet temperature of 347.8 °C. However the considered application requires that this temperature should be kept below 330 °C. Work has been carried out to optimise the cycle with regard to this specific constraint through several options including the modification of the operating conditions and the investigation of other cycle configurations. The recompression cycle in condensing mode is finally identified as the most interesting one since it achieves an efficiency of 45.7% and features an optimal IHX inlet temperature of 328.6 °C.

* Corresponding author.
E-mail addresses: hong-son.pham@cea.fr (H.S. Pham), nicolas.alpy@cea.fr (N. Alpy), jean-henry.ferrasse@univ-amu.fr (J.H. Ferrasse), olivier.boutin@univ-amu.fr (O. Boutin), johann.quenaut@power.alstom.com (J. Quenaut), mark.tothill@power.alstom.com (M. Tothill), david.haubensack@cea.fr (D. Haubensack), manuel.saez@cea.fr (M. Saez).

Nomenclature

h	specific enthalpy (J/kg)
i	specific irreversibility (J/kg)
p	pressure (Pa)
q	heat per unit mass (J/kg)
Q	thermal power (W)
s	specific entropy (J/kg/°C)
T	temperature (°C)
w	specific work (J/kg)
x	specific transferred exergy (J/kg)
y	flow split ratio

Greek symbols

η	efficiency (turbomachinery & cycle)
ε	effectiveness (heat exchanger)
ψ	specific exergy (J/kg)

Subscripts

IHX	IHX inlet (temperature of CO_2)
in	inlet (of the main compressor)
max	maximum (pressure)
[n](s)	state point (of an isentropic process)
o	state of the reference environment
r	state of the reference heat source
recup	recuperation (power)
thermal	thermal (efficiency)
exergy	exergy (efficiency)

Abbreviations

BC	bypass compressor
CSP	concentrated solar power
HTR	high temperature recuperator
IC	intercooled recompression cycle
LTR	low temperature recuperator
PC	partial-cooling cycle
sc-CO_2	supercritical CO_2
SMR	small modular reactor
TB	turbine
CL	CooLer
FSR	flow split ratio
HX	Heat eXchanger
IHX	intermediate heat exchanger
MX	mixer
RC	recompression cycle
SFR	sodium-cooled fast reactor
RH	ReHeated recompression cycle
TIT	turbine inlet temperature

1. Introduction

Thermal to mechanical energy conversion can be performed through a thermodynamic cycle whose performance is limited by the efficiency of the theoretical Carnot cycle. Today, the Rankine steam cycle is the dominant technology for power plants in operation, including all concentrated solar, biomass, coal-fired and nuclear power plants. It offers high efficiency due to a low ratio of input work for liquid phase pumping to output work from vapour phase expanding under a high pressure ratio. As an alternative, the closed Brayton cycle promotes operation at higher temperature, thereby potentially achieving higher efficiency. Nevertheless, the closed Brayton cycle requires large energy input for the compression process and therefore is only attractive in the very high temperature range, over 850 °C. In the high temperature range, around 500 °C, while less efficient than the Ranking cycle, it could be selected to accommodate other engineering/project constraints. For example, a Brayton nitrogen cycle is currently considered as an alternative to the conventional steam cycle for SFRs (sodium-cooled fast reactors) to avoid issues related to the fast and energetic sodium/water reaction [1].

A thermodynamic cycle using sc-CO_2 as the working fluid was claimed to avoid most of problems of the Rankine steam and other Brayton gas cycles while retaining many of their advantages [2–5]: (i) potentially high efficiency due to the low compression work required in the reduced compressibility region near the critical point; (ii) remarkably smaller size of the turbomachinery resulting from the high density and low heat capacity of the working fluid; (iii) simpler system layout than the Rankine steam cycle; (iv) less sensitive to the system pressure losses than other Brayton gas cycles; (v) better match of the temperature profile in the IHX (Intermediate Heat eXchanger) to that of the heat source in the supercritical region, compared to the case of a steam generator in the Rankine steam cycle. The past decade has seen a growing interest on the sc-CO_2 cycle through a significant amount of works that have been carried out in view of analysing these potential advantages for various heat sources such as: low-grade waste heat recovery applications [4], hybrid fuel cell systems [6], concentrated solar [7], nuclear reactors including innovative SMR (small modular reactor) [8], next generation nuclear reactors [5,9], and fusion reactor concepts [10,11]. Appendix A reports the diversity of the sc-CO_2 cycle configurations, operating conditions, as well as component efficiencies that have been used in these works.

The first configuration of the sc-CO_2 cycle, proposed by Feher, was a simple regenerative cycle [2]. This cycle suffers from large irreversibility due to the heat capacity imbalance between the hot and cold sides of the recuperator (i.e. the internal heat exchanger). To overcome this so-called pinch-point problem, Angelino introduced the RC (recompression) and PC (partial-cooling) cycles [3]. These cycles were initially proposed to operate in condensing mode. While reviewing the cycle relevancy for the Generation IV nuclear reactors application, Dostal et al. suggested switching the compression from the liquid region to the supercritical region in order to extend the application of this cycle to hotter heat-sink temperatures [5]. This change was also considered necessary to prevent crossing the critical temperature point during the compression process thereby avoiding any problem related to pump cavitation. Finally, reheat and intercooling, commonly used options for performance enhancement of the Brayton cycle, have been implemented in the sc-CO_2 cycle [7,12–14]. Schemes of each of these configurations are reported in Appendix B, together with a description of their physical mechanisms.

In the literature, in addition to the aforementioned diversity regarding cycle boundary conditions such as the heat sink temperature (see Appendix A), the thermodynamic analysis of the sc-CO_2 cycle has been performed considering different approaches. The first of these addresses considerations of the HXs (Heat eXchangers) performance during the optimisation process. In Refs. [5,8,12], component design and performance analyses were initially carried out for a reference cycle. Then, heat transfer and friction correlations, such as those given in Ref. [15], were used to determine the HXs performance at any set of operating conditions.

The resultant of such an approach is that the off-design performance of the cycle components interferes with the optimisation process. On the other hand, other works such as in Refs. [16–18] considered identical engineering targets for HXs effectiveness and pressure losses. Following this approach, the cycle is optimised without considering at first component dimensions, which are then calculated in a second step in order to check engineering relevancy of the cycle design in terms of compactness and performance. Another difference relates to how the FSR (flow split ratio), which is defined as the ratio of the main compressor mass flow rate to the total mass flow rate, is considered in the recompression and partial-cooling cycles. It is clear that the FSR has a strong effect on cycle performance and also on the temperature difference between the two fluid streams entering the mixing point. In some reference works, it was seen as a variable to be calculated in order to have a zero temperature difference [5,7,17]. Another approach was to treat the FSR as an operating condition, being optimised for highest efficiency regardless of this temperature difference [1,8,12]. Alternatively, according to results in Ref. [13], simultaneous optimisation of the FSR, main compressor inlet pressure and reheat stage outlet pressure made this temperature difference tend to zero for a reheated recompression cycle at a TIT (turbine inlet temperature) of 550 °C and a maximum pressure of 20 MPa. However, this result has not been verified in other works. For instance, the recompression cycle in Ref. [12] featured a temperature difference of 12 °C at the mixing point. It cannot therefore be generalised for all cycle configurations operating at various conditions.

Under these diverse considerations, works have been performed to determine the highest efficiency of the cycle through optimisation of the operating conditions. However, the optimisation depends on constraints regarding the specific application since the temperature of the CO_2 entering the cold side of the IHX must be kept below that of the primary fluid leaving the hot side. Indeed the latter has to be limited to comply with peculiar constraints of the considered application such as relaxation of the mechanical stress of the reactor vessel for a nuclear application. This requirement, hereafter called IHX temperature constraint, becomes more important as the sc-CO_2 cycle features a small temperature change through the IHX. This is driven by a small temperature drop in the turbine. In contrast the optimum cycle efficiency is found for a highly recuperated design, the CO_2 entering the IHX has to be effectively preheated through a recuperator [19]. This constraint may prevent the CO_2 temperature leaving the IHX, i.e. the TIT, from reaching the maximum possible value which reflects the heat source temperature. For example, a TIT of 415 °C was reported in Ref. [12] for the reheated recompression cycle when coupled to the Advanced Burner Test Reactor which featured an available heat source temperature of around 480 °C. The cycle efficiency dropped 2 points compared to that of the reference recompression cycle. Later, the partial-cooling cycle was coupled to the Very High Temperature Reactor concept which gave a TIT of 661 °C, far below the temperature of the reactor coolant entering the IHX at 850 °C [19]. Consequently, this deficient TIT resulted in a thermal efficiency of 47.9% compared to 57% of the cycle without considering any constraint.

The results from the above reported review and data compiled in Appendix A show that a variety of approaches have been considered in the literature for cycle configurations, component performance, optimisation strategies, and constraints. This prevents one from having a consistent view of the sc-CO_2 cycle thermodynamic potential as a function of the heat source temperature. The current study first addresses this point by evaluating the performance of the sc-CO_2 cycle under a unique set of the aforementioned considerations. The maps of thermal efficiency, optimal IHX inlet temperature (in the following, IHX inlet temperature or T_{IHX} refers to the CO_2 temperature at the IHX inlet), and recuperation power (i.e. the thermal power transferred through two recuperators) have been presented for different cycle configurations. These charts could be considered as a first engineering guideline on the maximum potential of the sc-CO_2 cycle for a given TIT. However, as mentioned above, this data will then have to be revised to encompass the requirements of any specific application, in particular the IHX temperature constraint. Accordingly, the present work addresses specific optimisations for two nuclear applications of interest, namely an SMR and an SFR concept. Exergy analysis has been carried out since it provides a meaningful assessment of individual component efficiencies and allows one to identify locations of and respective magnitudes of losses.

2. Materials and methods

2.1. Exergy analysis

Exergy represents the upper limit of the amount of work a system can deliver without violating any thermodynamic law as it comes to equilibrium with a reference environment. On the contrary to energy, exergy is not a conserved but a destroyed quantity in any real process. Exergy destruction is proportional to the entropy created due to irreversibility associated to the process. In Ref. [20], the concept of exergy was integrated into a practical method of thermodynamic analysis for thermal power plants.

Exergy analysis, through quantification of the exergy destruction, identifies the location and magnitude of the irreversibilities in a system. Since this approach measures the deviation of the considered process from the ideal one, it provides a more meaningful evaluation of the system efficiency and so eases cycle comprehension when compared to the energy analysis. General methods for formulating the performance criteria of specific thermal plants are outlined in Ref. [21]. A comprehensive review of its application on the thermal power plants can be found in Ref. [22] while concrete examples are given in Refs. [23,24].

Accordingly, the specific irreversibility is calculated through the exergy transferred by heat, by work and by mass (per unit mass) for any control volume:

$$i = \Sigma x_{heat} + \Sigma x_{mass} + \Sigma x_{work} = \Sigma q(1 - T_o/T_r) + \Sigma\psi + \Sigma w \qquad (1)$$

where the specific exergy at each state is determined by:

$$\psi = h - h_o - T_o(s - s_o) \qquad (2)$$

Applying this approach to the sc-CO_2 recompression cycle, specific irreversibility of the components, as well as energy balance used in traditional energy analysis, is given in Table 1. It is assumed that the cycle operates in steady state with no heat loss, except heat rejection to the environment through the cooler. State coordinates of the thermodynamic points are referred to the T-s diagram of the

Table 1
Energy balance and specific irreversibility of the sc-CO_2 recompression cycle components. Subscripts denote cycle components and thermodynamic state points shown in Fig. 1.

Component	Energy balance	Specific irreversibility
TB	$w_{TB} = h_1 - h_2$	$i_{TB} = \psi_1 - \psi_2 - w_{TB}$
MC	$w_{MC} = y(h_6 - h_5)$	$i_{MC} = y(\psi_5 - \psi_6) + w_{MC}$
BC	$w_{MC} = (1-y)(h_7 - h_4)$	$i_{BC} = (1-y)(\psi_4 - \psi_7) + w_{BC}$
HTR	$h_2 - h_3 = h_{10} - h_9$	$i_{HTR} = (\psi_2 - \psi_3) + (\psi_9 - \psi_{10})$
LTR	$h_3 - h_4 = y(h_8 - h_6)$	$i_{HTR} = (\psi_3 - \psi_4) + y(\psi_6 - \psi_8)$
CL	$q_{CL} = y(h_4 - h_5)$	$i_{CL} = y(\psi_4 - \psi_5)$
MX	$h_9 = (1-y)h_7 + yh_8$	$i_{MX} = (1-y)\psi_7 + y\psi_8 - \psi_9$
IHX	$q_{IHX} = h_1 - h_{10}$	$i_{IHX} = \psi_{IHX} + \psi_{10} - \psi_1$

recompression cycle (cf. Fig. 1). IC (intercooled recompression), RC (reheated recompression), and partial-cooling cycles have been analysed through the same principles.

The specific exergy input to the cycle via heat transfer in the IHX is given by:

$$\psi_{IHX} = q_{IHX}(1 - T_o/T_r) \tag{3}$$

The exergy efficiency of the cycle is defined as the ratio of exergy output to the exergy input through the IHX:

$$\eta_{Exergy} = (w_{TB} - w_{MC} - w_{BC})/\psi_{IHX} = 1 - (\Sigma i)/\psi_{IHX} \tag{4}$$

It can be linked to the thermal efficiency through the theoretical Carnot efficiency:

$$\eta_{Thermal} = \eta_{Exergy}\eta_{Carnot} \tag{5}$$

in which:

$$\eta_{Thermal} = (w_{TB} - w_{MC} - w_{BC})/q_{IHX} \tag{6}$$

$$\eta_{Carnot} = 1 - T_o/T_r \tag{7}$$

2.2. Cycle modelling tool

In CYCLOP (CYCLe OPtimisation) [25], the CEA tool for power conversion cycle modelling, a cycle is represented by a set of fluid loops built from different components (heat source and sink, turbomachines, heat exchangers) which are described by macroscopic parameters such as efficiency (or effectiveness), pressure and heat losses if not adiabatic, and mass flow rate. Components are connected by points where thermodynamic states (temperature, pressure) are stored. This tool solves automatically the mass and energy balances for all components of the cycle from a minimum set of input data, allowing all cycle parameters to be quickly modified and optimised using the well-known deterministic Nelder-Mead algorithm [26]. CYCLOP has been validated on Rankine steam cycles coupled to French Pressurized Water Reactors (such as CRUAS) and the French SFR Superphenix. It has also been extensively benchmarked in the frame of R&D programs, from the helium Brayton cycle applied to a Gas-cooled Fast Reactor concept [25] to the sc-CO_2 cycle for an SFR [16]. In this code, the CO_2 properties are determined from the Helmholtz free energy equation of state [27]. This equation is considered by the National Institute of Standards and Technology as being the most accurate one to describe the thermodynamic properties of CO_2 for a wide range of scientific and engineering applications.

3. Results and discussions

3.1. sc-CO_2 cycle performance mapping

The mapping of the thermodynamic performance has been performed for the recompression cycle, the reheated recompression cycle, the intercooled recompression cycle, and the partial-cooling cycle under a set of conditions and component performance given in Table 2. The CO_2 temperature is maintained constant at the inlet of the two turbines of the reheated recompression cycle. Similarly, the temperature of the CO_2 leaving the pre-cooler of the partial-cooling cycle and the inter-cooler of the intercooled recompression cycle is always kept equal to that at the cooler outlet, chosen to be 35 °C in order to conveniently adapt to various environments. As the cycle is considered for different applications and hence for different thermal powers, pressure losses could not be relevantly sized and thus are not taken into account at this stage. An additional constraint is implemented in the optimisation tool concerning the pinch temperatures in the recuperators. Indeed, it is supposed that a minimum internal pinch temperature of 10 °C is a conservative engineering choice to ensure that the design of these HXs is technologically achievable.

Figs. 2 to 5 plot the TIT dependency of the optimal thermal efficiency, the corresponding IHX inlet temperature, the optimal main compressor inlet pressure and the recuperation power for different cycle configurations. The maximum pressure is a parameter and has been set at 20 and 25 MPa. The recuperation power is normalised by the thermal power of the heat source. The legends RC, RH, IC, and PC represent the recompression, reheated recompression, intercooled recompression and partial-cooling cycles, respectively. From these figures, several conclusions can be made for each configuration when compared to the reference recompression cycle:

- The reheated recompression cycle shows a gain in efficiency over the whole range of turbine inlet temperatures investigated. A greater improvement in efficiency can be seen at lower TITs than at higher TITs. The reheat stage increases noticeably the optimal temperature of the CO_2 entering the IHX. This configuration is therefore convenient for applications featuring a low temperature rise across the IHX. However, the required

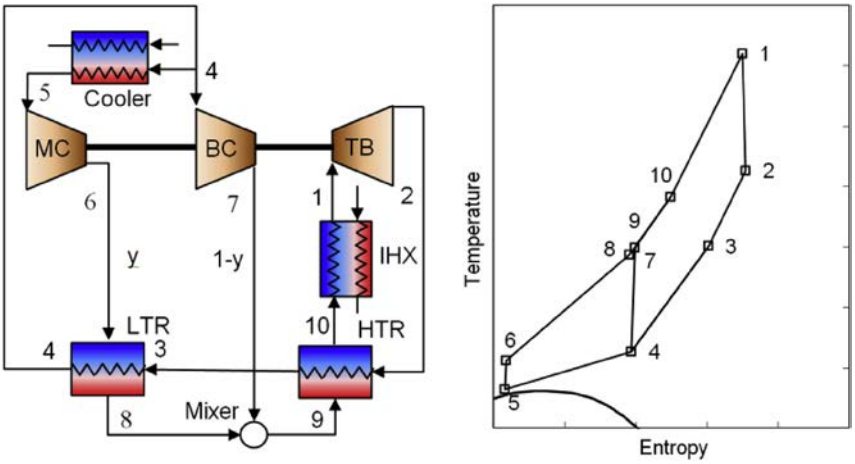

Fig. 1. The sc-CO_2 recompression cycle and its T-s diagram.

Table 2
Cycle operating conditions and components performances used to produce the maps of the sc-CO_2 cycle thermodynamic performance.

TIT (°C)	250–850
P_{max} (MPa)	20; 25
T_{in} (°C)	35
η_{TB}	93%
η_{MC}	88%
η_{BC}, η_{PC}, η_{IC}	87%
ε_{HTR}, ε_{LTR}	≤92.5%
Recuperators pinch temperature, °C	≥10
Pressure losses, MPa	0

recuperation power is higher, leading to larger and more expensive components.

- Intercooling also provides performance enhancement but less noticeable than reheat. It also slightly reduces the optimal IHX inlet temperature. The recuperation power of the intercooled recompression cycle is similar to that of the recompression one at low temperatures. It remains constant regardless the change of TIT above 550 °C for the 25 MPa cycle and slowly increases above 450 °C for the 20 MPa cycle.
- The partial-cooling cycle is less efficient than the recompression cycle over the range of TIT studied for the 25 MPa cycle. As the TIT increases, the efficiency gap reduces. For a maximum cycle pressure of 20 MPa and for turbine inlet temperatures above 700 °C the performance of the partial-cooling cycle exceeds that of the recompression cycle. In addition, this configuration decreases the optimal IHX inlet temperature, thereby promoting its coupling to applications featuring a large temperature rise through the primary side of the IHX. One more advantage is that significantly lower recuperation power is required by the partial-cooling cycle.

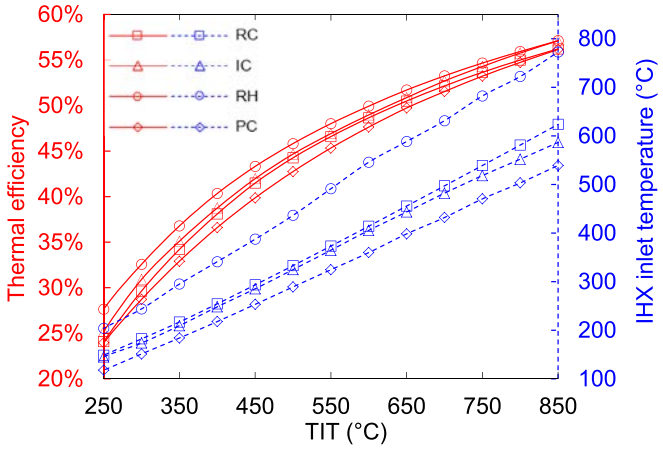

Fig. 2. TIT dependency of the thermal efficiency and optimal IHX inlet temperature of different optimised 25 MPa sc-CO_2 cycles.

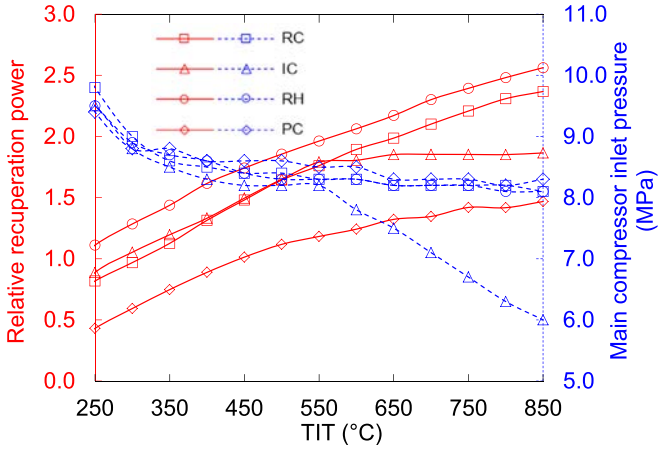

Fig. 3. TIT dependency of the relative recuperation power and main compressor inlet pressure of different optimised 25 MPa sc-CO_2 cycles.

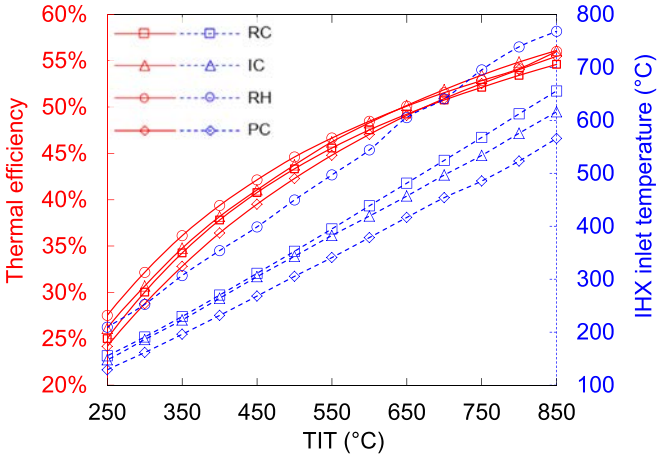

Fig. 4. TIT dependency of the thermal efficiency and optimal IHX inlet temperature of different optimised 20 MPa sc-CO_2 cycles.

The particular trend in the recuperation power of the intercooled recompression cycle at high TITs can be explained by the fact that its optimal efficiency is connected to a remarkable decrease of the main compressor inlet pressure (i.e. increase of the pressure ratio). Indeed, for a turbine operating under a given inlet pressure, an increase in the pressure ratio leads to a higher turbine work. This additional work is more important with the increase in TIT and can exceed the additional work required by the compressors. This is the case of the intercooled recompression cycle in which the additional work of the compressors is relaxed thanks to the intercooling. A higher pressure ratio leads to a lower temperature at the turbine outlet and therefore to lower recuperation power.

3.2. *sc-CO_2 cycle study for an SMR*

Research on the innovative SMR concept has been the subject of much interest in the recent years. Typically featuring an electric

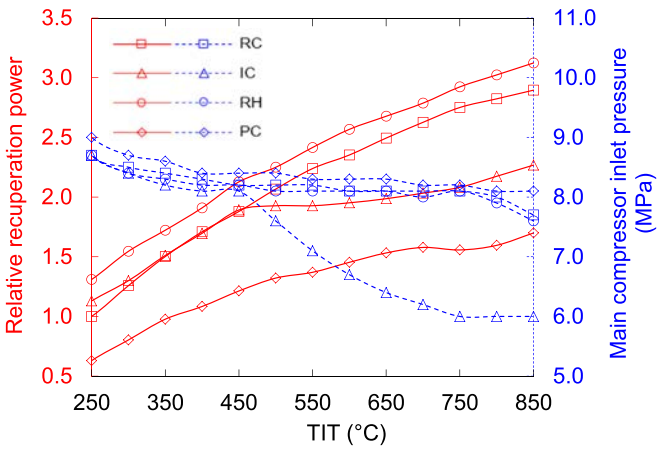

Fig. 5. TIT dependency of the relative recuperation power and main compressor inlet pressure of different optimised 20 MPa sc-CO_2 cycles.

power below 300 MWe, an SMR is designed for applications in remote or isolated areas where electrical grids are poorly developed or absent. It can also be used to cogenerate non-electrical products such as heat or desalinated water [28]. The key advantage of innovative SMR concept is that it could be manufactured and assembled in factories before being transported to the power plant site. This strategy reduces the on-site construction time and cost. At ALSTOM, an R&D program to investigate the optimum power conversion system suitable for SMR applications is being pursued. The sc-CO_2 cycle is being investigated as an optional power conversion system to reinforce the modular-ability and footprint minimisation. Current reactors suitable for SMR application feature reactor coolant temperatures of 306 °C and 271 °C at the IHX inlet and outlet respectively, giving a constant TIT of 275 °C.

Table 3 recaps some data picked up from the plots shown in Figs. 2–5 at 275 °C TIT. There is little performance improvement or even a degradation by increasing the maximum pressure from 20 to 25 MPa. Intercooling adds 0.8 point efficiency to the 20 MPa recompression cycle while reheating enhances it by 2.3 points. Moreover, the reheated recompression cycle features a higher IHX inlet temperature, which better matches the reactor coolant temperature at the IHX outlet and thus would be convenient for the IHX design.

Regarding the recuperation power, its variation is in line with the change of the turbine outlet temperature. The latter depends on the pressure ratio: higher pressure ratio leads to lower turbine outlet temperature and thus to lower recuperation power. Hence, the recuperation power of the 25 MPa cycle is lower than that of the 20 MPa cycle for a considered configuration. Compared to the recompression cycle, the reheated cycle features higher turbine outlet temperature and thus higher recuperation power. On the contrary, the lower recuperation power of the partial-cooling cycle results from its higher pressure ratio. The intercooling cycle, since it features lower temperature at the main compressor outlet, has lower temperature of CO_2 leaving the hot side of the LTR (low temperature recuperator), and thereby higher recuperation power.

3.2.1. Parametric study of the sc-CO_2 recompression cycle coupled to an SMR

Cycle performance dependency on the FSR has been first investigated, setting the main compressor inlet and outlet pressures at 8.4 and 20 MPa, respectively. The remaining conditions are taken as being the same as in Table 2. However for this application a 0.3 MPa total pressure drop value is used. An exergy analysis has been performed with the reference heat source and reference environment temperatures of 306 °C and 20 °C, respectively. Component irreversibility (cf. Fig. 6) has been made relative to the exergy input to the cycle. As previously concluded in Ref. [3], irreversibility in the turbomachines is small compared to that in the heat exchangers. Additionally, since FSR is considered as a parameter to be optimized, it comes out that flow splitting is an effective

Table 3
Optimal performance of different cycle configurations at a TIT of 275 °C. Recuperation power is normalised to the thermal power of the heat source. For the RH cycle, the temperatures at the inlet of both IHXs are given.

Cycle	P_{max} (MPa)	$\eta_{thermal}$	Q_{recup}	T_{IHX} (°C)
RC	20	27.5%	1.13	173.1
	25	26.8%	0.92	166.2
IC	20	28.3%	1.19	168.1
	25	28.1%	0.97	159.4
RH	20	29.8%	1.43	206.8/230.8
	25	30.1%	1.21	200.7/225.7
PC	20	26.5%	0.72	145.1
	25	26.3%	0.51	134.5

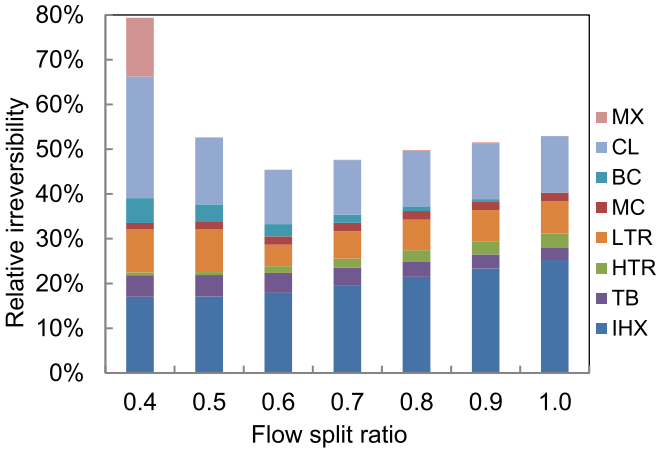

Fig. 6. FSR dependency of the components irreversibility of the 20 MPa recompression cycle coupled to an SMR at 8.4 MPa compressor inlet pressure.

way to reduce the irreversibility in the HTR (high temperature recuperator) and LTR, as well as in the IHX and cooler. However, too small a FSR reverses the evolution of the irreversibility in the LTR and cooler. This also leads to significantly large irreversibility in the mixer. Therefore, an optimal FSR must satisfy the compromise of these opposite trends to achieve the highest efficiency, as illustrated in Fig. 7.

The influence of the compressor inlet pressure on the thermal efficiency and on the recuperation power is illustrated in Fig. 8. The thermal efficiency changes slightly with any increase of the compressor inlet pressure for the 25 MPa case: there is only 0.35 point efficiency change as the minimum cycle pressure varies from 8.6 to 10 MPa. Such behaviour could favour a cycle design in region of smother change of CO_2 properties, i.e. far from the critical point, without considerable decrease of its performance. It complies with any possible implication on the stability of the cycle that might occur in the region of sharp change of CO_2 properties. One can therefore consider it to be a safe and efficient engineering choice. Nevertheless, cycle operation at low compressor inlet pressure is an interesting option in term of system compactness since lower recuperation power is required. If stable operation of the sc-CO_2 cycle closer to the critical point can be demonstrated, such a choice would therefore lead to save component costs and system

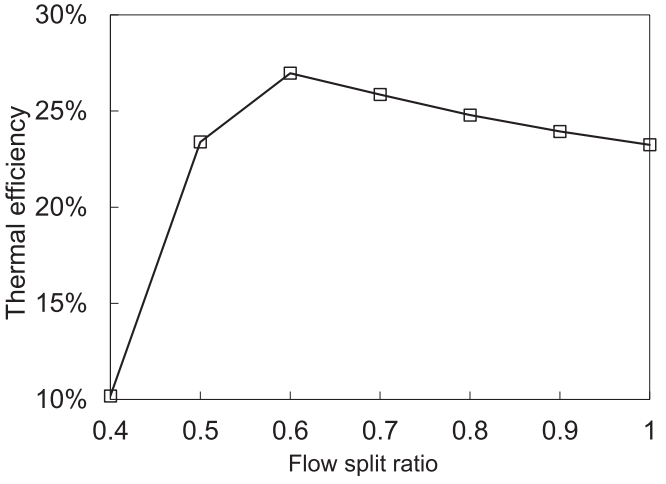

Fig. 7. FSR dependency of the thermal efficiency of the 20 MPa recompression cycle coupled to an SMR at 8.4 MPa compressor inlet pressure.

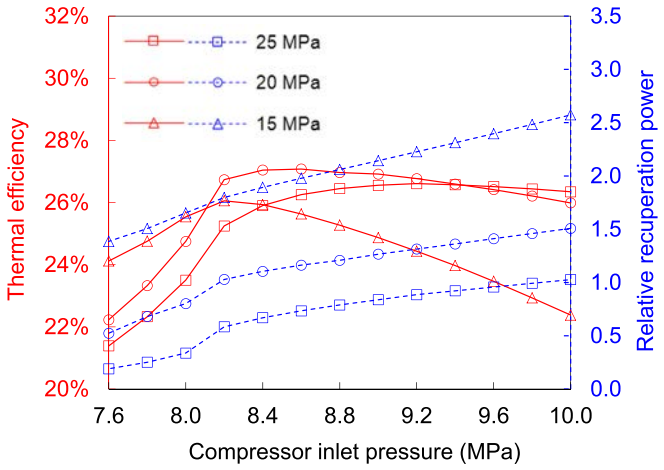

Fig. 8. Thermal efficiency and relative recuperation power as functions of compressor inlet pressure of the 15, 20, and 25 MPa recompression cycles coupled to an SMR.

footprint. This is the path which is followed in the next paragraph which addresses further cycle optimisation. A 20 MPa maximum pressure will be considered since it has been highlighted to offer the most efficient cycle (cf. Fig. 8).

3.2.2. *Performance improvement of the sc-CO_2 cycle coupled to an SMR*

Exergy analysis shows that flow splitting and main compressor inlet pressure optimisation can remove most of the irreversibility in the HTR and LTR. The large irreversibility remaining in the IHX and cooler highlights possible directions for performance improvement of the sc-CO_2 cycle. As indicated by the plots shown in Fig. 4, one approach would be to add a reheat stage to the recompression cycle, since this decreases IHX irreversibility. A second way to increase the sc-CO_2 recompression cycle efficiency would be by operating it in condensing mode to decrease cooler irreversibility. This latter point supposes the availability of a low heat sink temperature giving a compressor inlet temperature of 27 °C. This will be used in the following analysis.

Components' irreversibilities of the optimal recompression and reheated recompression cycles are plotted in Fig. 9. Irreversibilities in the two IHXs of the reheated recompression cycle are encapsulated together in a 'joined IHX' to ease comparison with the

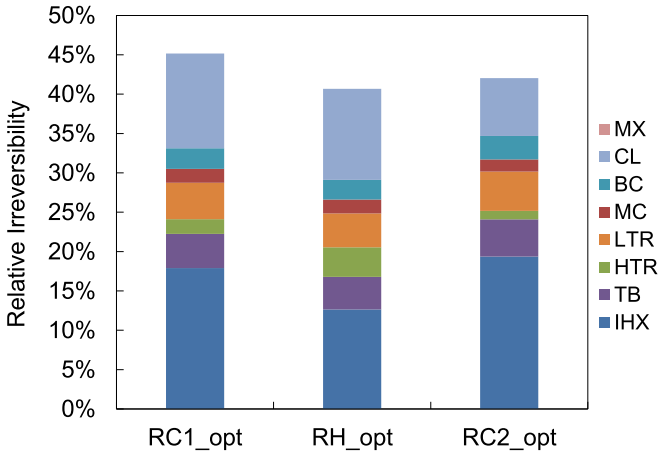

Fig. 9. Components relative irreversibility of different optimised 20 MPa sc-CO_2 cycles coupled to an SMR. RC1_opt, RC2_opt, and RH_opt stand for the recompression, recompression in condensing mode, and reheated recompression cycles, respectively.

recompression cycle. Data related to the operating conditions and the potential of each cycle are reported in Table 4. A similar practice is applied for the two turbines. The 'joined IHX' features lower irreversibility compared to that of the recompression cycle, thereby leading to a thermal efficiency enhancement of 2.2 points. For the recompression cycle in condensing mode, slightly higher irreversibility has been found in the IHX but it is compensated with much lower irreversibility in the cooler. Hence, an efficiency gain of 1.5 points has been achieved. More details on the operating conditions of this cycle can be found in Appendix C.

These two options are therefore highlighted as affording performance enhancement. The reheat option has been considered and rejected by ALSTOM as adding too much complexity and footprint to the power conversion system. Hence, at this stage, the operation in condensing mode has been identified as being the most promising of the sc-CO_2 cycles for an SMR application, although the penalty compared to a Rankine cycle is significant, about 5 points. The preliminary study on the SMR plant layout using this sc-CO_2 cycle has demonstrated that a potential footprint saving of around 20% on the turbine hall could be achieved when compared to a typical turbine hall with a Rankine cycle of the same duty (cf. Table 5). This reduction is possible because the equipment for sc-CO_2 plant is much more compact than the equipment for conventional steam plants. The simplicity of this Brayton cycle also makes it suitable for modularisation and off-site module preparation so that minimum assembly work would be required on site. Final step on this preliminary study is to compare the cost of electricity between a conventional steam turbine plant and the sc-CO_2 plant to better understand if the simplicity and the compactness of this solution could actually counterbalance the loss in performance.

Figs. 10–12 illustrate a comprehensive view of the sc-CO_2 recompression cycle potential for various inlet operating conditions of the main compressor, covering liquid, gas, and supercritical regions. The optimal performance path between RC1_opt and RC2_opt also provides some trends about the minimum cycle performance degradation due to seasonal change of the heat sink temperature. The real deviation would be defined through an off-design study of the cycle with a thermohydraulic system code as performed in Ref. [16] with the Plant Dynamics Code from Argonne National Laboratory [29]. In support to condensing mode, which has been reported as the most promising cycle design, further studies are planned to consider the risk of possible cavitation of the main compressor as well as the off-design behaviour of this component through the liquid and supercritical regions.

3.3. *sc-CO_2 cycle study for an SFR*

The SFR is one of the six chosen concepts of the next generation nuclear reactors intended to be in industrial operation after 2040

Table 4
Summary of operating conditions and performance of different optimised sc-CO_2 cycles coupled to an SMR. Cycle labels are the same as in Fig. 9. Recuperation power is normalised to the thermal power of the heat source. For the RH cycle, the temperatures at the inlet of both IHXs are given.

	RC1_opt	RH_opt	RC2_opt
P_{max}, MPa	20	20	20
T_{in}, °C	35	35	27
P_{in}, MPa	8.6	8.53	7.33
P_{int}, MPa	N/A	13.22	N/A
FSR	0.602	0.609	0.566
Q_{recup}	1.16	1.45	0.99
T_{IHX}, °C	173.9	206.4/232.6	163.4
η_{exergy}	54.8%	59.3%	58.0%
$\eta_{thermal}$	27.1%	29.3%	28.6%

Table 5
Preliminary sizing of the turbine hall of the SMR plant layout with the Rankine steam cycle and the sc-CO_2 cycle.

	Steam cycle	sc-CO_2 cycle
Turbomachinery volume, m^3	96	61
Length of shaftline including alternator (+length of co-axial exhaust), m	33	24
Volume of heat exchangers (excluding heater/steam generator & cooler/condenser, outside turbine hall), m^3	276	209
Turbine hall length, m	54	46
Turbine hall width, m	32	30
Turbine hall footprint, m^2	1730	1380
Maximum height component, m	12.5	7.0

[30]. Criteria for the selection of these reactors address uranium natural resources sustainment, radioactive waste minimisation, skills for economic competitiveness and robustness with respect to non-proliferation and malicious acts. They will also be required to possibly comply with the emergence of new applications, such as hydrogen production or water desalination. Studies on the sc-CO_2 cycle are currently viewed as part of the long term R&D program for French SFR deployment [1]. The application of the sc-CO_2 cycle to an SFR test case was previously considered in Refs. [1,16,31]. The latest work reported a thermal efficiency of 43.9% for the 25.3 MPa recompression cycle at a TIT of 515 °C and an optimal IHX inlet temperature of 347.8 °C. Recent study [32] has shown that a sodium temperature of 345 °C leaving the hot side of the IHX could interestingly enhance the compactness of the vessel and sodium intermediate loop. Such a case will require a typical IHX inlet temperature of the power conversion cycle below 330 °C. The study hereafter reported aims to match the sc-CO_2 cycle with this new requirement.

Table 6 picks up data from the plots shown in Figs. 2–5, providing the performance of different cycle configurations at a TIT of 515 °C. Here, the thermal efficiency of the optimised recompression cycle is higher than the result 43.9% in Ref. [16] because HXs and pipes pressure losses are not accounted for. Among all configurations, only the partial-cooling one satisfies the IHX temperature constraint. Another benefit is that a significant reduction in recuperation power has been obtained. However, it provides lower efficiency than the reference recompression cycle.

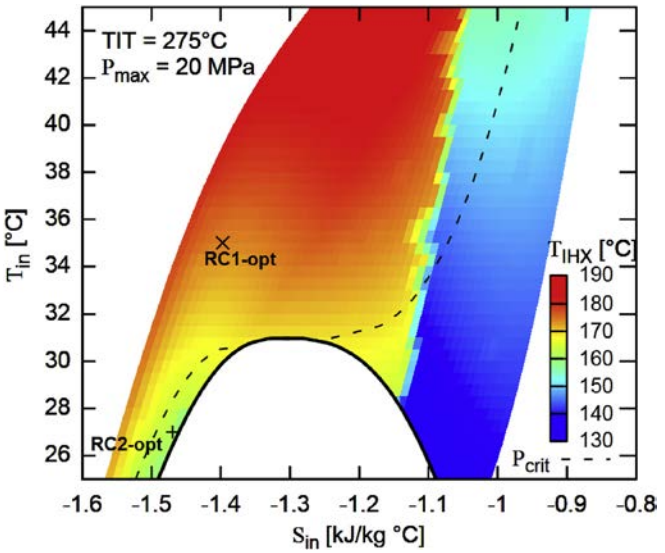

Fig. 11. IHX inlet temperature chart of the 20 MPa sc-CO_2 recompression cycle coupled to an SMR at various main compressor inlet conditions. Dotted line represents the critical pressure line.

3.3.1. *Parametric study of the sc-CO_2 recompression cycle coupled to an SFR*

A thermodynamic analysis has been performed at a TIT of 515 °C and maximum pressures of 15.3, 20.3, and 25.3 MPa. Components performances are similar to those shown in Table 2, except that a total pressure drop of 0.55 MPa has been taken into account. In addition, the 10 °C recuperators pinch point temperature constraint has been found to be naturally satisfied and thereby having no impact on the optimisation process. Indeed, these analysis conditions are taken same as those employed in Ref. [16] to ease comparison.

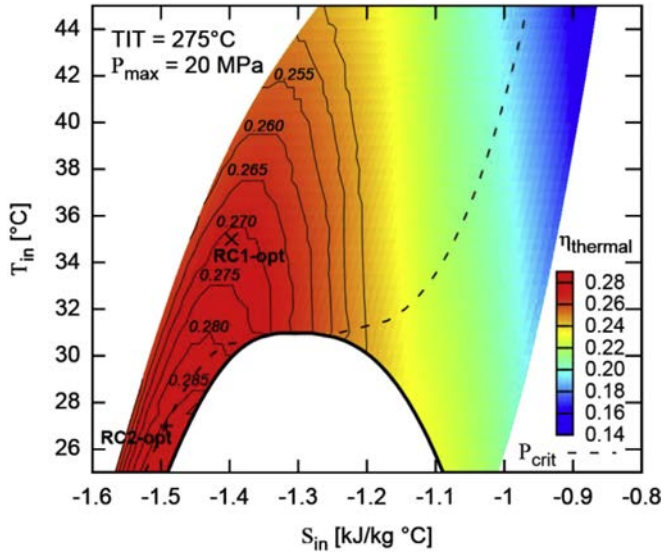

Fig. 10. Efficiency chart of the 20 MPa sc-CO_2 recompression cycle coupled to an SMR at various inlet operating conditions of the main compressor. Dotted line represents the critical pressure line.

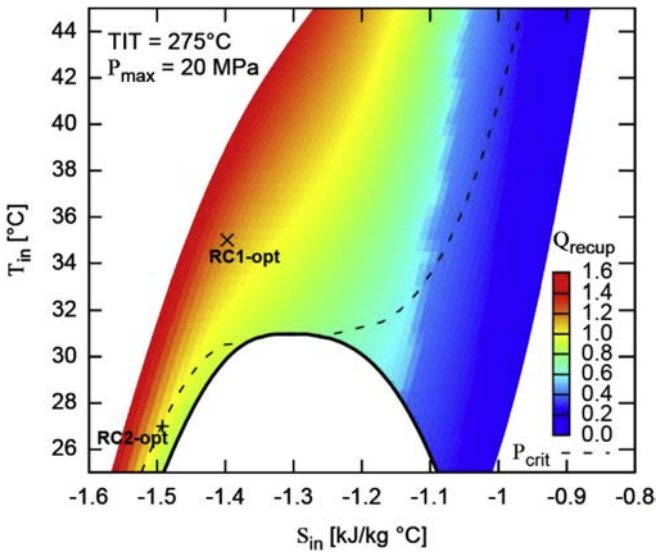

Fig. 12. Relative recuperation power chart of the 20 MPa sc-CO_2 recompression cycle coupled to an SMR at various main compressor inlet conditions. Dotted line represents the critical pressure line.

Table 6
Summary of the performance of different sc-CO_2 cycle configurations at the TIT of 515 °C. Recuperation power is normalised to the thermal power of the heat source. For the RH cycle, the temperatures at the inlet of both IHXs are given.

Cycle	P_{max} (MPa)	$\eta_{thermal}$	Q_{recup}	T_{IHX} (°C)
RC	20	44.0%	2.12	365.3
	25	45.0%	1.68	345.0
IC	20	44.5%	1.91	354.4
	25	45.3%	1.69	336.8
RH	20	45.2%	2.28	408.3/466.9
	25	46.5%	1.88	394.9/455.7
PC	20	43.0%	1.33	315.5
	25	43.5%	1.14	299.8

Investigation of component irreversibility and recuperation power dependency on flow split ratio and main compressor inlet pressure led to the same observations than those reported for the SMR case. Impact of these parameters on thermal efficiency and optimal IHX inlet temperature are plotted in Figs. 13 and 14. A noticeable point, when compared to the SMR case, is the significant sensitivity of thermal efficiency to changes in the main compressor inlet pressure. The efficiency of the 25.3 MPa cycle reduces by 1.6 points when the compressor inlet pressure is increased from 8.6 MPa to 10 MPa. For the 25.3 MPa cycle, it cannot be expected to match the IHX temperature constraint by changing the main compressor inlet pressure around its optimal value. However, an effective way for this purpose should consist in increasing the FSR above its optimal value. The next paragraph reports how this change degrades cycle performance and investigates alternative possibilities.

3.3.2. Investigating possibilities to comply with the IHX temperature constraint of an SFR test case

The partial-cooling cycle has been highlighted in Table 6 as an efficient way to satisfy the IHX temperature constraint. This could also be achieved by modifying the operating conditions of the recompression and intercooled recompression cycles. In addition to increasing the FSR, decreasing the TIT, as shown in Fig. 4, or increasing the maximum pressure, as suggested in Table 6, will reduce the IHX inlet temperature. However, a higher maximum pressure than 25 MPa would require further consideration of the mechanical constraints. Hence, the current investigation considers TIT as the only additional parameter to be optimised. The IHX temperature constraint is fulfilled by mathematically adding this criterion along the optimisation process. The operation of the recompression cycle in condensing mode will also be considered as previously done in the case of the SMR. Note that since the reheated

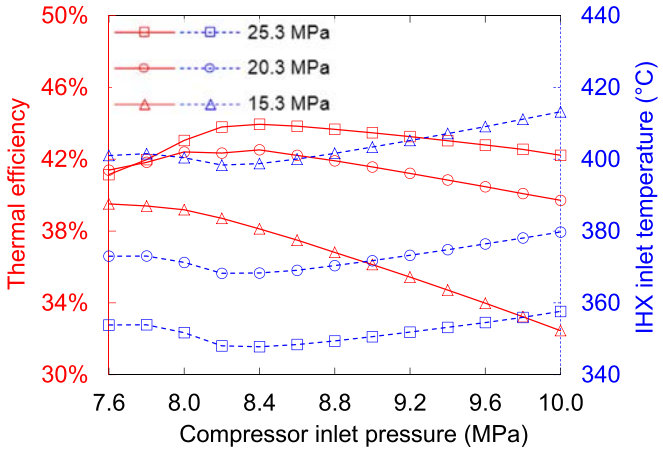

Fig. 13. Thermal efficiency and IHX inlet temperature as functions of main compressor inlet pressure of the 15.3, 20.3, and 25.3 MPa recompression cycles coupled to an SFR.

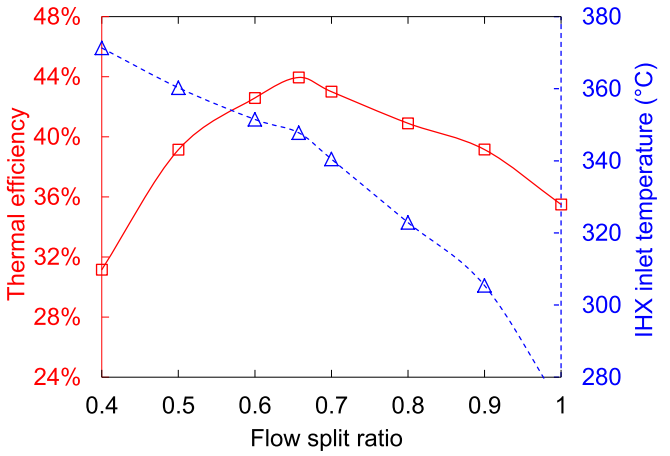

Fig. 14. FSR dependency of the thermal efficiency and IHX inlet temperature of the 25.3 MPa recompression cycle coupled to an SFR at 8.4 MPa compressor inlet pressure.

recompression cycle significantly increases the IHX inlet temperature it is excluded from this investigation.

On this basis, an exergy analysis has been performed with 530 °C and 20 °C as the reference heat source and environment temperatures, respectively. Component irreversibility for each cycle is plotted in Fig. 15. Table 7 reports data related to the operating conditions as well as the performance of each cycle. As previously described in section 3.3.2, the inter-cooler/pre-cooler and cooler are represented by a 'joined cooler' as are the inter-compressor/pre-compressor and the main compressor.

Consistent with the previous discussion, the optimised recompression cycle with the IHX temperature constraint features higher FSR (flow split ratio) and smaller TIT than those of the original recompression cycle (i.e. cycle without the IHX temperature constraint). With the decrease of TIT, from 515° to 497 °C, larger irreversibility in the IHX has been observed. The cycle efficiency has been found to decrease to 42.6%, compared to 43.9% for the original cycle.

The partial-cooling cycle has a much lower IHX inlet temperature, 303 °C, than the requirement of 330 °C and has the same performance as the optimised recompression cycle with the IHX temperature constraint. This could be seen as an interesting point since it likely reduces the heat transfer area and thus the IHX size. A

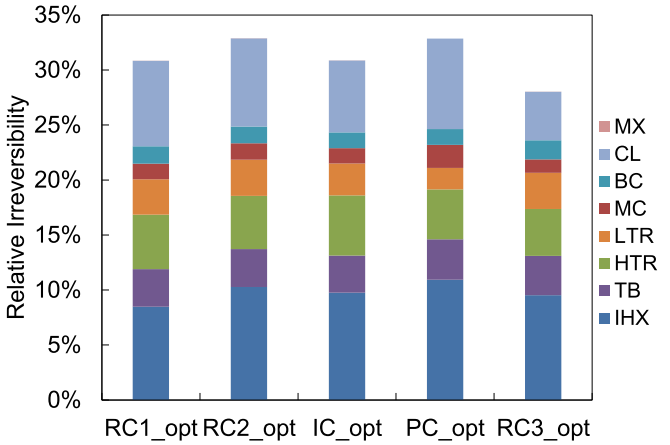

Fig. 15. Components relative irreversibility of different optimised 25.3 MPa cycles coupled to an SFR. RC1_opt, RC2_opt, and RC3_opt respectively stand for the optimised recompression cycles with and without the IHX temperature constraint, and the optimised recompression cycle operating in condensing mode. IC_opt and PC_opt represent the optimised intercooled recompression and partial-cooling cycles.

Table 7
Operating conditions and performance of different optimised cycles coupled to an SFR. Recuperation power is normalised to the thermal power of the heat source. Cycle labels are the same as in Fig. 15. P_{min} and P_{int} stand for the minimum pressure of the partial-cooling cycle and the pressure at the inlet of the intercooling stage of the intercooled recompression cycle, respectively.

	RC1_opt	RC2_opt	IC_opt	PC_opt	RC3_opt
TIT, °C	515	496.9	508.2	515	515
P_{max}, MPa	25.3	25.3	25.3	25.3	25.3
T_{in}, °C	35	35	35	35	27
P_{in}, MPa	8.40	8.34	8.10	8.51	7.08
P_{min}, MPa	N/A	N/A	N/A	5.87	N/A
P_{int}, MPa	N/A	N/A	10.77	N/A	N/A
FSR	0.657	0.674	0.662	0.565	0.627
Q_{recup}	1.73	1.63	1.66	1.14	1.51
T_{IHX}, °C	347.8	330.0	330.0	302.7	328.6
η_{exergy}	69.1%	67.1%	69.1%	67.1%	72.0%
$\eta_{thermal}$	43.9%	42.6%	43.9%	42.6%	45.7%

similar advantage could benefit the recuperators, as previously mentioned, due to small recuperation power.

The intercooled recompression cycle, characterised by a larger IHX temperature rise, experiences less decrease in TIT than the optimised recompression cycle with the IHX temperature constraint. However, this change leads to a very small reduction of IHX irreversibility. Nevertheless, a significant improvement has been found in the 'joined cooler' which operates at a lower average temperature thanks to the additional intercooling stage. The intercooled recompression cycle does indeed achieve the same performance as the original recompression cycle while assuring the IHX temperature constraint.

The operation of the recompression cycle in condensing mode results in lower irreversibility in the cooler. The IHX inlet temperature is slightly below the aforementioned limit, thereby avoiding large irreversibility in the IHX, as experienced in the partial-cooling cycle (cf. Fig. 15). The highest efficiency has therefore been achieved in this case. Additionally, the recuperation power is attractively lower than that of the recompression cycle operating entirely in the supercritical region. More details on the operating conditions of this cycle can be found in Appendix C. As for the SMR, the recompression cycle in condensing mode is identified as the most interesting option for the SFR among others.

4. Conclusions

The mapping of the thermodynamic performance of the sc-CO_2 cycle as a function of the TIT has been performed in a 250−850 °C range for different cycle configurations. Reheat offers the recompression cycle higher efficiency, especially at low TIT, and narrows the optimal temperature change along the IHX. The use of intercooling for the main compressor does not significantly increase the performance but slightly increases the IHX temperature change and the recuperation power of the cycle in the high temperature range. The partial-cooling cycle is not as efficient as the recompression cycle but requires smaller recuperation power. Such a design is also convenient for applications featuring large IHX temperature change. Given these observations, the established charts can be used as a preliminary guideline to assess the thermodynamic performance and suitability of the sc-CO_2 cycle for any considered application.

The current generation SMR has been selected as a typical application of the cycle in a low heat source temperature range. Parametric studies have highlighted that the efficiency of the recompression cycle changes slightly in a wide range of the main compressor inlet pressure. Accordingly, a higher pressure can be selected to ensure operation of the cycle further from the critical point, where large fluid property gradients take place. Lower pressure, however, provides smaller recuperation power and thereby allows a reduction in the recuperator volume. A maximum efficiency of 27.1% has been found for the recompression cycle. Two options for performance enhancement have been investigated. The reheated recompression cycle offers a thermal efficiency of 29.3% while the operation in condensing mode increases the efficiency to 28.6%. Even though the penalty compared to a Rankine steam cycle is significant, around 5 points, the latter is viewed as an interesting option since it offers system simplicity and footprint saving.

In the high temperature range, a specific study has been carried out to design the sc-CO_2 cycle for an SFR test case. A lower IHX inlet temperature of 330 °C, compared to the optimal value of 347.8 °C for an original recompression cycle, was targeted. This additional constraint makes the cycle thermal efficiency decrease from 43.9% to 42.6%. As an alternative, the partial-cooling cycle which is found to comply with the new specification, provides the same 42.6% efficiency but requires much lower recuperation power. The intercooled recompression cycle produces an efficiency of 43.9% but requires higher recuperation power than the original recompression cycle. Operating the recompression cycle in condensing mode, at a compressor inlet temperature of 27 °C, is identified as the most interesting option since the cycle achieves the highest efficiency (45.7%) and the recuperation power remains smaller than that of the original recompression cycle.

Appendix A

Table A1 reports the diversity of cycle configurations, operating conditions and components performances that have been used to

Table A1
Compiled data from some published works on the thermodynamic optimisation of the sc-CO_2 cycle coupled to various applications. Acronyms: CSP: Concentrated Solar Power, FC: Fuel cell, GFR: Gas-cooled Fast Reactor, G4R: 4th generation nuclear reactor, N/A: not applicable, SC: Simple regenerative Cycle, VHTR: Very High Temperature Reactor, WHR: Waste Heat Recovery, 3-RC: Cascades of three sc-CO_2 recompression cycles. (a) Off-design HXs performance was interfered with the optimisation process. (b) FSR was calculated to reach zero temperature difference at the mixing point. (c) Reheat was also examined as a performance enhancement option to the partial-cooling cycle.

Ref.	Application	Configuration	TIT (°C)	P_{max} (MPa)	P_{min} (MPa)	T_{min} (°C)	FSR	η_{TB} %	η_{MC} %	η_{BC} %	ε_{HTR} %	ε_{LTR} %	$\eta_{thermal}$ %
[33]	WHR	SC	215	24.6	8.96	37.8	N/A	85	85	N/A	80	N/A	N/A
[8] (a)	SMR	RC	310	15	7.70	32	0.54	90	89	89	N/A	N/A	29.0
[12] (a)	SFR	RC	472	20	7.62	32.8	0.71	93.4	88.9	87.9	91.7	94.5	39.1
[34]	SFR	RC	508	20	7.40	31.2	0.71	93.4	89.1	87.5	91.7	94.6	42.8
[16]	SFR	RC	515	25.3	8.36	35	0.66	93.0	88.0	87.0	92.5	92.5	43.9
[5] (a, b)	G4R	RC	550	20	7.69	32	0.59	90	89	89	96.3	92.1	45.3
[9]	GFR	RC	550	20	7.69	32	0.59	94.2	91.1	90.5	N/A	N/A	47.2
[9]	GFR	RC	650	20	7.69	32	0.59	94.2	91.1	90.5	N/A	N/A	51.3
[6]	FC	SC	650	22.5	7.50	35	N/A	95.0	90.0	N/A	95.0	N/A	39.1
[19] (a)	VHTR	3-RC	830	20	7.62	32.8	0.69	91.4	90.6	90.3	95.1	96.6	49.5
[13] (b)	N/A	RH	550−750	20−30	N/A	32	N/A	90	85	85	86	86	N/A
[17] (b)	N/A	SC, RC, PC	500−850	25	N/A	32	N/A	93	90	90	95	95	N/A
[7] (b) (c)	CSP	RC, RH, PC	500−850	25	N/A	45 & 60	N/A	93	89	89	95	95	N/A

analyse the potential advantages of the scCO$_2$ cycle for various applications.

Appendix B

The simple regenerative cycle

The first proposed sc-CO$_2$ cycle is a simple regenerative cycle, operating entirely above the critical pressure with the compression performed in the liquid region [2]. Its configuration is similar to the

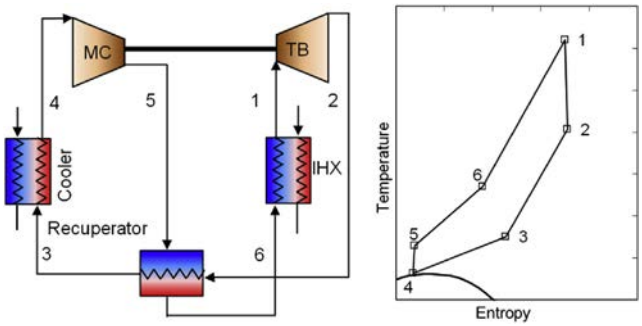

Fig. A1. The simple regenerative sc-CO$_2$ cycle and its T-s diagram. Note that the compressor inlet conditions are shifted to near the critical point in the T-s diagram compared to the original cycle of Feher [2].

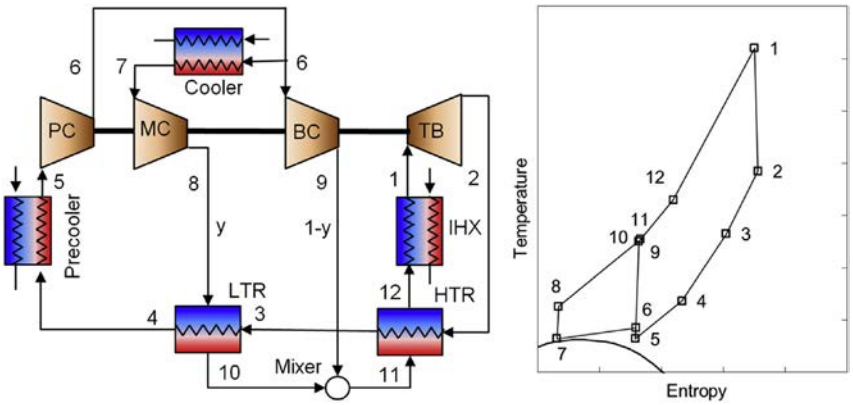

Fig. A2. The partial-cooling sc-CO$_2$ cycle proposed by Angelino [3] and its T-s diagram.

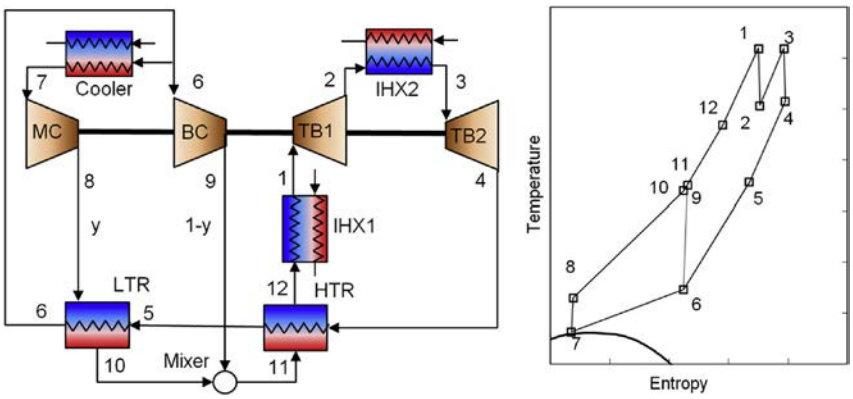

Fig. A3. The reheated recompression sc-CO$_2$ cycle with reheat and its T-s diagram.

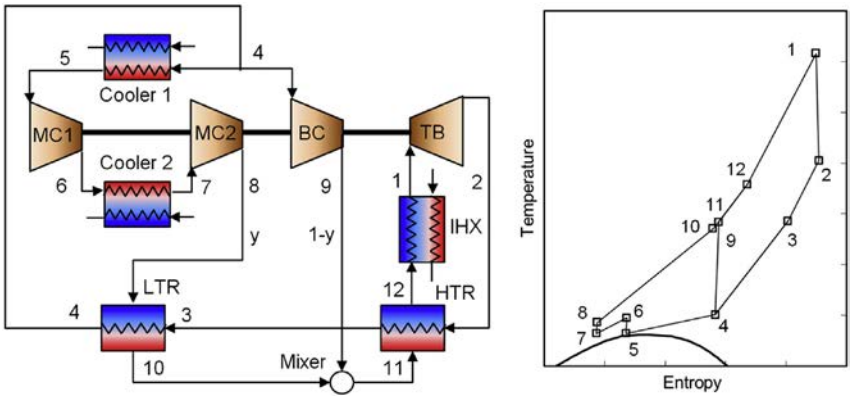

Fig. A4. The intercooled recompression sc-CO_2 cycle and its T-s diagram.

regenerative Brayton gas closed-cycle (cf. Fig. A1). Due to real gas behaviour of CO_2 near the critical point, heat capacity depends not only on temperature but also on pressure. In the recuperator, heat capacity of the low pressure hot stream (2–3) is much smaller than that of the high pressure cold stream (5–6). Because of this imbalance, large temperature difference and thus large irreversibility is found in the recuperator.

The recompression cycle

In the recompression cycle (cf. Fig. 1), heat capacity imbalance between the hot and cold streams is overcome by sending only a fraction of the flow through the cold side of the LTR. The rest of the flow, split before entering the cooler (4), passes through the bypass compressor. These two high pressure streams are then mixed (9) before passing the HTR. Note that flow splitting is characterised by the FSR which is the ratio of the mass flow rate across the cooler to the total mass flow rate.

The partial-cooling cycle

The recompression cycle, even though it could eliminate the pinch point problem, has low flexibility on the turbine exhaust pressure since this latter is also the main compressor inlet pressure (if one neglect pressure losses). Indeed, this pressure should be accommodated with temperature so that operation of the main compressor will remain in the thermodynamic region of interest, i.e. affording a reduced compression work. To make the turbine outlet pressure independent of the compressor inlet pressure, a pre-compressor, combined with a pre-cooler, was introduced before the splitting point (6). The low pressure flow leaving the hot side of the LTR (4) is pre-cooled before entering the pre-compressor throughout which it is compressed to the main compressor inlet pressure. The rest of the cycle is similar to the recompression cycle. The partial-cooling cycle therefore experiences higher expansion ratio and thus higher turbine specific work. This extra work is expected to be high enough to compensate the additional work required for pre-compressor operation so that net output work of the cycle would be promoted.

The recompression cycle with reheat and intercooling

Reheat and intercooling are commonly used options to improve the performance of a Brayton gas cycle. They make the expansion and the compression closer to isothermal processes (see Carnot's ideal cycle). Otherwise speaking, reheat increases the specific work given by the turbine and intercooling decreases work consumed by the compressor. Efficiency gain could therefore be expected.

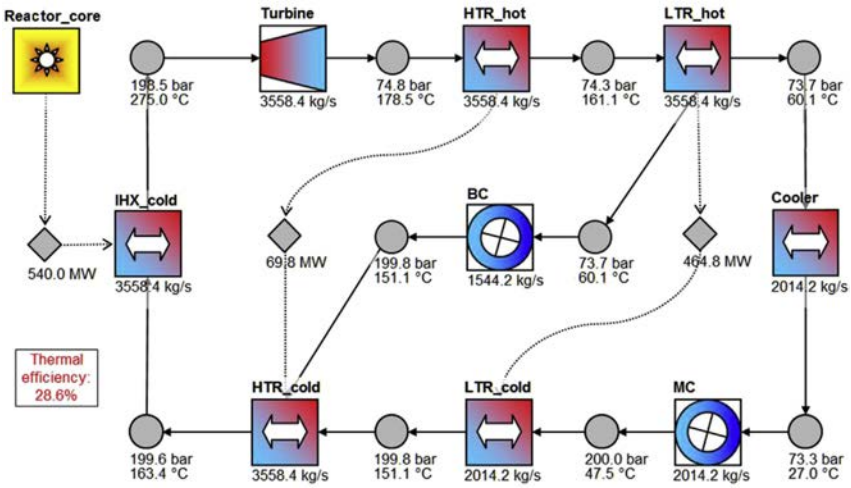

Fig. A5. CYCLOP scheme of the optimised sc-CO_2 recompression cycle in condensing mode coupled to an SMR.

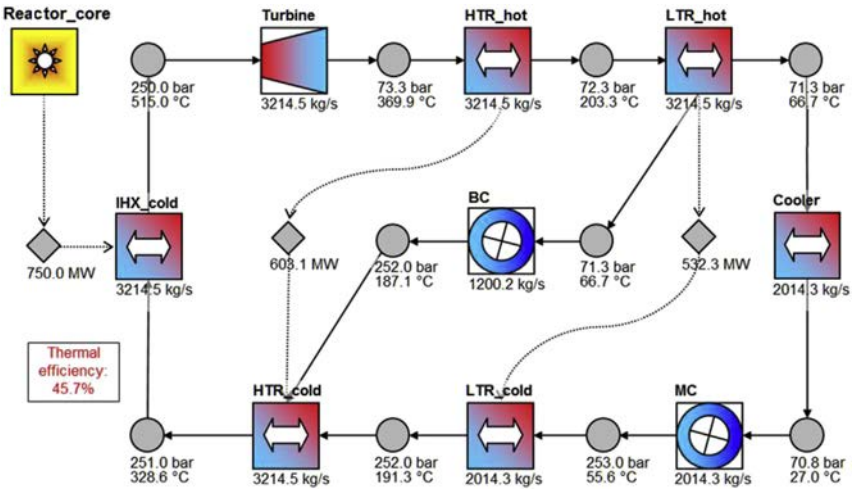

Fig. A6. CYCLOP scheme of the optimised sc-CO_2 recompression cycle in condensing mode coupled to an SFR.

Appendix C

Figs. A5 and A6 show the CYCLOP schemes of the optimised sc-CO_2 recompression cycles in condensing mode for an SMR and an SFR. Therein, hot and cold sides of each heat exchanger are modelled separately and the heat transfer is represented by dotted lines. Pressure and temperature are indicated under each node and mass flow rate is given under each component.

References

[1] Alpy N, Haubensack D, Simon N, Gicquel L, Rodriguez G, Cachon L. Gas cycle testing opportunity with ASTRID, the French SFR prototype. In: Proceeding of the 2011 Supercritical CO_2 Power Cycle Symposium, Boulder, Colorado; 2011.

[2] Feher EG. The supercritical thermodynamic power cycle. Energy Convers 1968;8(2):85–90.

[3] Angelino G. Carbon dioxide condensation cycles for power production. J Eng Power 1968;90(3):287–95.

[4] Chen Y. Thermodynamic cycles using carbon dioxide as working fluid: CO_2 transcritical power cycle study [Dissertation]. KTH Royal Institute of Technology; 2011.

[5] Dostal V, Driscoll MJ, Hejzlar P. A super critical carbon dioxide cycle for next generation nuclear reactors. Massachusetts Institute of Technology. Center for Advanced Nuclear Energy Systems; Mar. 2004. Advanced Nuclear Power Program, Technical Report, Available at: web.mit.edu/22.33/www/dostal.pdf.

[6] Sanchez D, Chacartegui R, Jimenez-Espadafor F, Sanchez T. A new concept for high temperature fuel cell hybrid systems using supercritical carbon dioxide. J Fuel Cell Sci Technol 2009;6(2).

[7] Turchi CS, Ma Z, Neises TW, Wagner MJ. Thermodynamic study of advanced supercritical carbon dioxide power cycles for concentrating solar power systems. J Sol Energy Eng Jun. 2013;135(4):041007.

[8] Yoon HJ, Ahn Y, Lee JI, Addad Y. Potential advantages of coupling supercritical CO_2 Brayton cycle to water-cooled small and medium size reactor. Nucl Eng Des 2012;245:223–32.

[9] Hejzlar P, Dostal V, Driscoll MJ, Dumaz P, Poullennec G, Alpy N. Assessment of gas-cooled fast reactor with indirect supercritical CO_2 cycle. Nucl Eng Technol 2006;38(2):436–46.

[10] Sardain P, Maisonnier D, Medrano M, Brañas B, Puente D, Arenaza E, et al. Alternative power conversion cycles for He-cooled fusion reactor concepts. In: Proceedings of the 2nd IAEA Technical Meeting on First Generation of Fusion Power Plants: Design and Technology, Vienna, Austria; 2007.

[11] Ishiyama S, Muto Y, Kato Y, Nishio S, Hayashi T, Nomoto Y. Study of steam, helium and supercritical CO_2 turbine power generations in prototype fusion power reactor. Prog Nucl Energy Mar. 2008;50(2–6):325–32.

[12] Moisseytsev A, Sienicki JJ. Investigation of alternative layouts for the supercritical carbon dioxide Brayton cycle for a sodium-cooled fast reactor. Nucl Eng Des Jul. 2009;239(7):1362–71.

[13] Sarkar J, Bhattacharyya S. Optimization of recompression S-CO_2 power cycle with reheating. Energy Convers Manag Aug. 2009;50(8):1939–45.

[14] Muto Y, Kato Y. Cycle thermal efficiency of supercritical CO_2 gas turbine dependent on recuperator performance. J Power Energy Syst 2013;7(3):148–61.

[15] Ngo TL, Kato Y, Nikitin K, Ishizuka T. Heat transfer and pressure drop correlations of microchannel heat exchangers with S-shaped and zigzag fins for carbon dioxide cycles. Exp Therm Fluid Sci Nov. 2007;32(2):560–70.

[16] Floyd J, Alpy N, Moisseytsev A, Haubensack D, Rodriguez G, Sienicki J, et al. A numerical investigation of the sCO2 recompression cycle off-design behaviour, coupled to a sodium-cooled fast reactor, for seasonal variation in the heat sink temperature. Nucl Eng Des Jul. 2013;260:78–92.

[17] Kulhánek M, Dostál V. Thermodynamic analysis and comparison of supercritical carbon dioxide cycles. In: Supercritical CO_2 Power Cycle Symposium, Boulder, Colorado; 2011.

[18] Pérez-Pichel GD, Linares JI, Herranz LE, Moratilla BY. Thermal analysis of supercritical CO_2 power cycles: assessment of their suitability to the forthcoming sodium-cooled fast reactors. Nucl Eng Des Sep. 2012;250:23–34.

[19] Moisseytsev A, Sienicki JJ. Analysis of supercritical CO_2 cycle control strategies and dynamic response for generation IV reactors. Argonne National Laboratory; Apr. 2011. ANL-GENIV-124.

[20] Kotas TJ. Exergy concepts for thermal plant: first of two papers on exergy techniques in thermal plant analysis. Int J Heat Fluid Flow Sep. 1980;2(3):105–14.

[21] Kotas TJ. Exergy criteria of performance for thermal plant: second of two papers on exergy techniques in thermal plant analysis. Int J Heat Fluid Flow Dec. 1980;2(4):147–63.

[22] Kaushik SC, Reddy VS, Tyagi SK. Energy and exergy analyses of thermal power plants: a review. Renew Sustain Energy Rev May 2011;15(4):1857–72.

[23] Aljundi IH. Energy and exergy analysis of a steam power plant in Jordan. Appl Therm Eng Feb. 2009;29(2–3):324–8.

[24] Sarkar J. Second law analysis of supercritical CO_2 recompression Brayton cycle. Energy 2009;34(9):1172–8.

[25] Haubensack D, Thévenot C, Dumaz P. The copernic/cyclop computer tool: preconceptual design of generation 4 nuclear systems. In: Proceedings of the 2004 Conference on High Temperature Reactors, Beijing, China; 2004.

[26] Nelder JA, Mead R. A simplex method for function minimization. Comput J Jan. 1965;7(4):308–13.

[27] Span R, Wagner W. A new equation of state for carbon dioxide covering the fluid region from the triple-point temperature to 1100 K at pressures up to 800 MPa. J Phys Chem Ref Data 1996;25(6):1509.

[28] Kunetsov V, Lokhov A. Current status, technical feasibility and economics of small nuclear reactors. OECD Nuclear Energy Agency; Jun. 2011.

[29] Moisseytsev A, Sienicki J. Development of a plant dynamics computer code for analysis of a supercritical carbon dioxide Brayton cycle energy converter coupled to a natural circulation lead-cooled fast reactor. Argonne National Laboratory; Jul. 2006. ANL-06/27.

[30] Warin D, Rostaing C. Recent progress in advanced actinide recycling processes. Nuclear Energy Agency of the OECD; 2012.

[31] Floyd J, Alpy N, Haubensack D, Avakian G, Rodriguez G. On-design efficiency reference charts for the supercritical CO_2 Brayton cycle coupled to an SFR. In: Proceedings of the 2011 International Congress on Advances in Nuclear Power Plants (ICAPP'11), Nice, France; 2011.

[32] Cachon L, Biscarrat C, Morin F, Haubensack D, Rigal E, Moro I, et al. Innovative power conversion system for the French SFR prototype. ASTRID. 2012.

[33] Di Bella FA. Gas turbine engine exhaust waste heat recovery navy shipboard module development. In: Supercritical CO_2 Power Cycle Symposium, Boulder Colorado; 2011.

[34] Cha JE, Kim SO, Seong SH, Eoh JH, Lee TH, Choi SK, et al. Supercritical carbon dioxide Brayton cycle energy conversion system. KAERI, KAERI/TR-3500/2007. 2007.